

INTEGRATED STUDY OF THE INTERACTION BETWEEN GOLD NANORODS AND CANCER CELLS

UDC 61–006.6:612.017.1
Received 03.09.2014



V.V. Elagin, Research Worker, Scientific Research Institute of Biomedical Technologies¹; Postgraduate, the Department of Biomedicine²;

M.L. Bugrova, PhD, Head of Electron Microscopy Unit, Scientific Research Institute of Applied Fundamental Medicine¹;

E.N. Gorshkova, Junior Research Worker, Scientific Research Institute of Molecular Biology and Regional Ecology²;

E.A. Sergeeva, PhD, Senior Research Worker^{2,3};

E.V. Zagaynova, D.Med.Sc., Director of Scientific Research Institute of Biomedical Technologies¹; Head of the Department of Biomedicine²

¹Nizhny Novgorod State Medical Academy, Minin and Pozharsky Square, 10/1, Nizhny Novgorod, Russian Federation, 603005;

²Lobachevsky State University of Nizhni Novgorod — National Research University, Prospekt Gagarina, 23, Nizhny Novgorod, Russian Federation, 603950;

³Institute of Applied Physics of Russian Academy of Sciences, Ul'yanova St., 46, Nizhny Novgorod, Russian Federation, 603950

The aim of the investigation was to study the interaction of the gold nanorods stabilized by biocompatible agents with cancer cells.

Materials and Methods. The research was carried out on gold nanorods with extinction peak about 808 nm and 41×10 nm in size. Pluronic F127, chitosan and polyethylene glycol (PEG) solutions were used for stabilization. Optical characteristics of the solutions were investigated by a double-beam spectrophotometer. A cytotoxic effect of the nanoparticles was estimated by MTT assay. The interaction of the nanorods with eukaryotic cells was studied by two-photon luminescence microscopy and atomic force microscopy techniques. Transmission electron microscopy was used to perform a semi-quantitative analysis and study intracellular distribution.

Results. Stabilization of nanoparticles by Pluronic F127, chitosan and PEG resulted in the changes of their spectral characteristics with broadening of extinction peak and decrease of its intensity. All studied solutions of nanoparticles had the similar level of cytotoxicity. The nanoparticles found in cells were in the form of separate nanoparticles, larger assemblages and aggregates, the last two fractions prevailing. PEG-stabilized nanoparticles (after 1–3 h) and chitosan-stabilized nanoparticles (after 6 h) penetrated into cells the most efficiently. Endocytosis has been shown to play the main role in the internalization of nanoparticles.

Conclusion. The obtained results may lead to better understanding of the interaction process of nanomaterials with living cells, the influence of the stabilizing agent nature on optical properties of nanoparticles and their cytotoxic effects. Besides, the data on the accumulation of nanoparticles in cells will be useful when developing imaging techniques and therapy using nanomaterials.

Key words: gold nanoparticles; Pluronic F127; chitosan; polyethylene glycol; two-photon luminescence microscopy; transmission electron microscopy.

In recent years nanoparticles from various materials are widely used in a variety of spheres of human activity. In the industry they have found an application as catalytic components [1] and sensors [2]. Due to the ability to generate surface plasmon resonance and the related resonance absorption and scattering in a wide range of wavelengths in the biological “tissue optical window” [3, 4], nanoparticles are considered as theranostic agents [5]. They can serve as contrast agents [6] for laser nanosurgery [7] and cancer treatment [8], may be used for efficient target drug delivery [9], and also for control of cell functions [10]. Among a huge set of the nanoparticles received today, the rod-shaped gold nanoparticles are of great interest.

The spectrum of gold nanorods has two plasmon

resonance peaks. The first peak is located near a resonance of spherical nanoparticles (500–560 nm) and generally determined by the absorption of gold. The second peak is related to the longitudinal size of nanoparticles and easily adjusted by the axial ratio in a long-wave spectral range from 700 to 1300 nm, i.e. in “tissue optical window”. Nanorods are proved to convert electromagnetic energy of incident light into thermal energy [11, 12] much better compared to nanospheres. The abovementioned allows considering the nanorods as perspective agents for laser hyperthermia.

However, nanorods are known to penetrate into cells worse than spherical nanoparticles. B.D. Chithrani et al. [13] showed that cells take up nanorods 3–5 times less than spherical nanoparticles of the same size.

For contacts: Elagin Vadim Vyacheslavovich, e-mail: elagin.vadim@gmail.com

Moreover, short nanorods (length-width ratio is 1:1 and 1:3) penetrate into cells better than longer ones (1:5).

The use of the appropriate stabilizing agent may increase an effectiveness of the nanoparticles penetration into cell. The nanoparticles used in biomedical researches are stabilized by various biocompatible agents for aggregation prevention, decrease in toxicity and extension of the circulation time of the particles in the body. Most often Pluronic, chitosan and polyethylene glycol (PEG) are used.

Pluronic F127 is the block copolymer containing hydrophilic polyoxyethylene blocks and a hydrophobic polyoxypropylene block, with molecular weight of about 13 kDa. In dilute solutions with concentration of polymer above the critical micelle concentration the pluronic spontaneously forms micelles 30–50 nm in diameter, with a hydrophobic central core and hydrophilic residues directed towards the external surface [14, 15]. Due to this property, pluronic can be used for delivery of different drugs in the body including anticancer drugs [16].

Chitosan is a natural polysaccharide, the product of partial de-acetylation of chitin. Chitosan is capable to enhance the penetration of substances into tissues by opening of the dense epithelial contacts. Chitosan is also considered to increase cellular and intercellular transport in a mucous epithelium and other tissues [17, 18].

PEG is a water-soluble polymer that is widely used in biological researches. It is capable to decrease opsonization and an immune reaction of a body to the external agents and may prolong the time of their circulation. Free chains of the polymer sterically prevent aggregation of the nanoparticles and therefore stabilize them [19].

Investigation of interaction of nanoparticles with cells is carried out by high-resolution microscopy techniques, such as atomic-force microscopy (AFM) [20, 21], two-photon luminescent microscopy (TPLM) [22, 23], transmission (TEM) and scanning electron microscopies [13, 24]. For the quantitative assessment, atomic emission spectroscopy was used [25, 26]. AFM enables to detect the ultrastructural changes of cytoplasm membrane in the process of interaction with nanoparticles. An essential lack of the technique is possibility of obtaining the information only from an object surface. TPLM allows images of live cells to be obtained quickly and does not require special preparation of the samples. However, this technique does not allow visualization of separate nanoparticles or their localization in a cell, besides, during image acquisition it is necessary to control the power of the excitation laser in order to avoid melting of nanoparticles. TEM, on the one hand, enables to identify intracellular localization of nanoparticles and perform a semi-quantitative analysis of their content. On the other hand, it requires long time and special skills for the sample preparation. Atomic emission spectroscopy enables to identify the amount of the nanoparticles penetrated into cells, but requires specific preparation

of the sample and does not give any information about intracellular localization of nanoparticles. According to the aforesaid in the study AFM, TPLM and TEM were used.

The aim of the investigation was to study the interaction of the gold nanorods stabilized by biocompatible agents with cancer cells.

The study solved two problems: analysis of the influence of the stabilizing agents on spectral properties of nanoparticles, and the assessment of toxic effect of nanoparticles and dynamics of cellular uptake by high-resolution microscopy techniques.

Materials and Methods

Nanoparticles. The research was conducted on commercial gold nanorods 41×10 nm in size (Fig. 1, a) and with an absorption maximum on 808 nm (Sigma Aldrich, USA) (Fig. 1, b). Concentration of nanoparticles was approximately $5 \cdot 10^{11}$ particles/ml. Before the experiment the nanoparticles were washed from cetyltrimethylammonium bromide (CTAB) by centrifuging at 16 000 g within 10 min and by redispersion in Milli-Q water with the subsequent breaking of aggregates in an ultrasonic bath. This procedure was repeated 3 times, after that sediment of nanoparticles was re-dissolved in the solution of stabilizing agent. Pluronic F127 with final concentration in the solution of 2%, chitosan — 0.2% and PEG with a molecular weight 6 and 40 kDa — 3% were used for stabilization.

Spectral properties of the stock solution of nanoparticles and the solutions stabilized by the studied agents were analyzed by means of double-beam spectrophotometer Specord 250 (Analytik Jena AG, Germany) in the range of wavelengths of 400–1100 nm.

Cell culture. Cells of human ovary adenocarcinoma SKOV-3 (ATCC®, HTB-77™) were grown in culture dishes on RPMI-1640 medium (PanEko, Russia) with 10% fetal serum (HyClone, the USA) at 37°C and 5% of CO₂. 10^{11} nanoparticles stabilized by the studied agents were added in culture dishes 35 mm in diameter, the total volume of liquid being brought up to 2 ml culture medium. Cells with nanoparticles were maintained in the conditions of the CO₂ incubator within 1, 3 and 6 h, then the cells were triply washed from unbounded nanoparticles by PBS (PanEko, Russia). The cells stored for the same period of time and in the same conditions but without gold nanoparticles added were taken as control.

Cytotoxicity assessment. The influence of gold nanorods on viability of cells was carried out by MTT assay. For this purpose, cells were seeded on 96 well culture plates by 30 thousand cells per a well and after 6 h the solutions of nanoparticles were added. Cytotoxicity of stock solution of the nanoparticles stabilized by CTAB and solutions stabilized by Pluronic F127, chitosan, and PEG 6 kDa and 40 kDa, respectively, was investigated. In a plate well $5 \cdot 10^9$ and $5 \cdot 10^{10}$ nanoparticles were added and the total amount of the liquid was brought to 200 μ l by a culture medium. After 24 h the cells were washed

by 200 μ l of culture media without serum, followed by addition of 100 μ l of the MTT-solution (0.5 mg/ml), and plate stored in a CO₂ incubator within an hour without lid. After that, liquid in the wells was replaced on 100 μ l of dimethyl sulfoxide and the optical density at 570 nm by means of a microplate photometer SynergyMx (BioTek, USA) was measured. Values of optical density were averaged by three wells. Cells viability was represented as a percentage of the control ones, not treated by nanoparticles.

Atomic-force microscopy. By means of the AFM technique, changes of a relief of cell membrane induced treatment by gold nanorods were studied. For the research, cells were grown in 35 mm culture dishes within 24 h. Then 10¹¹ nanoparticles stabilized by the studied agents were added and the total volume of liquid was brought to 2 ml by a culture medium. Cells were incubated for 6 h in the conditions of CO₂ incubator and then fixed by 2.5% solution of glutaraldehyde on PBS buffer without washing free from nanoparticles.

Cell surfaces were studied by an atomic-force microscope SOLVER BIO™ (NT-MDT, Russia) using DNP (Veeco, USA) probes with radius of curvature about 50 nm, constant of rigidity of 0.58 N/m, resonant frequency in liquid about 40 kHz. Cantilever was placed on a special holder and lowered in the culture dish with cells located on an optical microscope. Scanning was processed with a speed of 0.5–1 line per second, the coefficient of a feed-back response being from 0.5 to 0.9. Set Point value was maintained around 55–60% of the initial value of oscillation frequency depending on the height of the studied cells. By means of the AFM technique, the sizes and borders of cells and nuclei, and quantity of the sites projecting over a membrane surface were assessed. In total 10 fields of view were analyzed. On the images presented in the work, lateral illumination that allows distinguishing in more detail roughnesses on a surface of the studied object was applied. The light source was located over a surface of cells at the left.

Two-photon luminescent microscopy. The penetration of gold nanoparticles in cancer cells was analyzed using Carl Zeiss LSM 510 META (Germany) laser scanning microscopy equipped with a femtosecond Ti:Sa laser. The pulse duration was 100 fs, pulse repetition rate — 80 MHz. In the experiments a laser was focused on the object by an oil immersion objective with a numerical aperture of NA=1.4. Two-photon excitation of gold nanoparticles was carried out at 810 nm which corresponded to the peak of the extinction coefficient of the gold nanorods (See Fig. 1, b). The excitation power was approximately 1 mW. Non-linear luminescence of gold nanoparticles was registered in the range of 501–565 nm selected according to the measurement spectrum of two-photon luminescence of nanoparticles. For visualization of cell borders we used a fluorescent marker of cell membranes CellMask™ (Life Technologies, USA), with excitation and emission maxima of 649 and 666 nm, respectively. For more information, three-dimensional images of samples were recorded. It should be noted that TPLM does not allow detecting separate nanoparticles because of the size and low level of luminescence signal. However, when agglomerates of nanoparticles are formed luminescence signal enhances and is easy to record [27]. By means of TPLM, the ability of nanoparticles to penetrate into cells depending on stabilizing agents was estimated.

Transmission electron microscopy. For the TEM-analysis the cells containing nanoparticles and cells without nanoparticles were harvested by trypsin/versene solution, washed once by PBS and transferred into eppendorfs. Suspension of cells was centrifuged for 5 min at 200 g. Cells sediment was fixed by 2.5% solution of glutaraldehyde on the phosphate buffer (pH=7.4) for 24 h followed by additional fixation by 1% osmium tetroxide solution for 1–2 h at +4°C. The samples were dehydrated in high-proof alcohol from 50 to 100%, and finally in 100% acetone. Further the cells

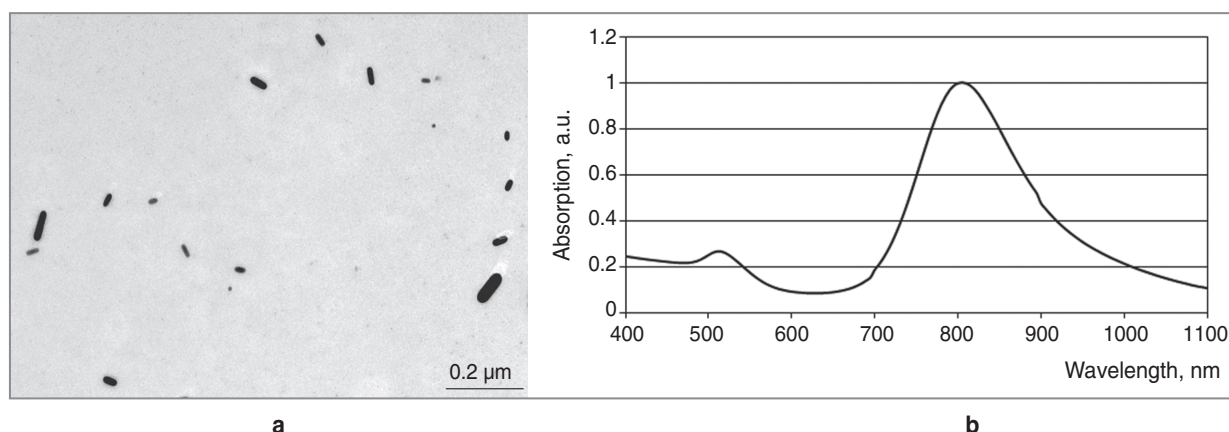


Fig. 1. Transmission electron microscopy of the nanoparticles solution (a) and extinction spectrum of the stock solution of nanoparticles (b)

were placed in the mixture of epoxide resin and pure acetone (1:1) for 24 h at room temperature. Then the samples were put into the mixture of epon-araldite for 24 h at 37°C followed by 24 h polymerization at 60°C [28]. Ultrathin sections (50–70 nm) were contrasted by uranyl acetate and analyzed by transmission electron microscope Morgagni 268D (FEI, USA). Nanoparticles in cells were visualized in 20 fields of view of 40×40 μm. By means of the TEM nanoparticles condition, intracellular distribution, and quantitative assessment was carried out. The results are presented in the form of summarized quantity of the nanoparticles found in cells in 20 fields of view.

Endocytosis research. According to the data [29, 30] the main role in the penetration of nanoparticles into cells is played by various mechanisms of endocytosis. For confirmation of endocytosis participation in the penetration of the nanoparticles stabilized by the studied agents, cells with nanoparticles were incubated at +4°C for 3 h. Endocytosis is an energy dependent process, so low temperature conditions decrease its intensity [31]. The presence of nanoparticles in cells was confirmed by the TPLM and TEM. Cells incubated with the same quantity of nanoparticles within 3 h at 37°C served as control.

Statistical processing of results. For analysis data, Statistica software, 10.0 was used (StatSoft Inc., USA). Statistically significant differences between control and experimental samples were revealed by Student's t-test for independent samplings. Mean rate of measured values and the standard deviations

were calculated. P<0.05 was considered statistically significant.

Results

Optical properties of nanoparticles. When preparing the solutions of gold nanorods stabilized by various agents, their optical properties were analyzed. Stock solution of nanoparticles had expressed peak of absorption at 808 nm. When washing nanoparticles of CTAB and stabilization by studied agents the broadening of absorption peak and decrease in its intensity (Fig. 2) was observed. It is established that stabilization by Pluronic F127 practically does not change spectrum of the nanoparticles. Stabilization by PEG 6 and 40 kDa and chitosan led to the broadening of the peak and decrease in its intensity indicating the formation of aggregates of nanorods.

Assessment of nanoparticles cytotoxicity. Using MTT assay we studied the viability of SKOV-3 cells treated by various concentrations of nanoparticles stabilized by the studied agents (Fig. 3). The diagram

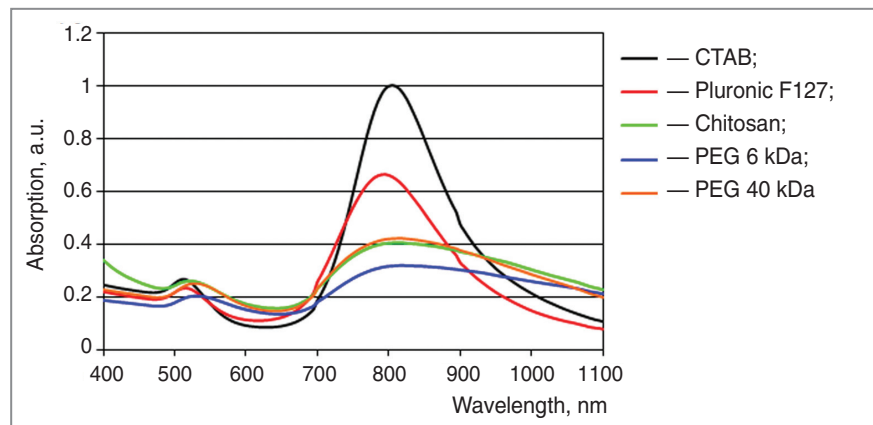


Fig. 2. Extinction spectra of the gold nanoparticles, stabilized by the studied agents

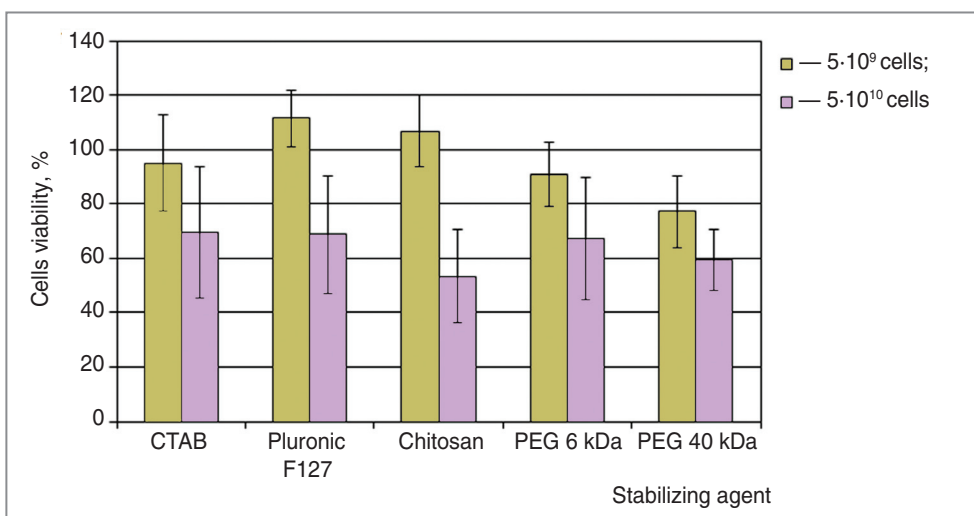


Fig. 3. Cells viability after 24 h of incubation with 5·10⁹ and 5·10¹⁰ nanoparticles, stabilized by Pluronic F127, chitosan, PEG 6 kDa, PEG 40 kDa and CTAB. The viability is presented as a percentage of the control

clearly shows the level of cytotoxicity of the stock solution of the nanoparticles stabilized by CTAB to be comparable with that for other solutions. Addition of $5 \cdot 10^9$ nanoparticles with CTAB to cells reduced their viability by no more than 10%, after $5 \cdot 10^{10}$ nanoparticles added the viability decreased to 70%. The nanoparticles stabilized by other agents also had cytotoxic effect on cell culture. The addition of $5 \cdot 10^{10}$ nanoparticles stabilized by chitosan in a plate well led to death of 55% of cells, whereas a smaller concentration of nanoparticles did not affect viability. Solution of the nanoparticles stabilized by Pluronic appeared to be the least toxic. The death of the cells did not exceed 30% if $5 \cdot 10^{10}$ nanoparticles were added. Nanoparticles stabilized by PEG 6 kDa reduced viability of cells by 35% in case of addition of $5 \cdot 10^{10}$ nanoparticles. The addition of $5 \cdot 10^9$ and $5 \cdot 10^{10}$ nanoparticles stabilized by PEG 40 kDa resulted in death of 20 and 40% of cells, respectively. Thereby, the nanoparticles, stabilized by chitosan or Pluronic F127 are the most suitable for biological studies.

Change of cell membranes. The analysis of the not treated (control) cells showed that they are rounded with a clear cell boundary on a substrate, and with a smooth cytoplasmic membrane (Fig. 4, a). After incubation with nanoparticles regardless of the type of a stabilizing agent, the structure of cells slightly changed. They were more elongated, besides, the borders of cell nuclei were less marked on surface. The incubation of cells with nanoparticles led to slight decrease in the sizes of cells and nuclei.

The analysis of the cells that have not been incubated with nanoparticles showed that on cell membranes there are about two sites, projected over a membrane surface. While the cells interacted with nanoparticles the quantity of such sites significantly increased, and the membrane invaginations appeared. The size of the sites found was from 100 nm to 5–6 μm (Fig. 4, b). For the nanoparticles stabilized by PEG 6 and 40 kDa, the maximum quantity of the sites was 27 and 24, respectively (Fig. 5). For the chitosan-stabilized nanoparticles 18 sites were

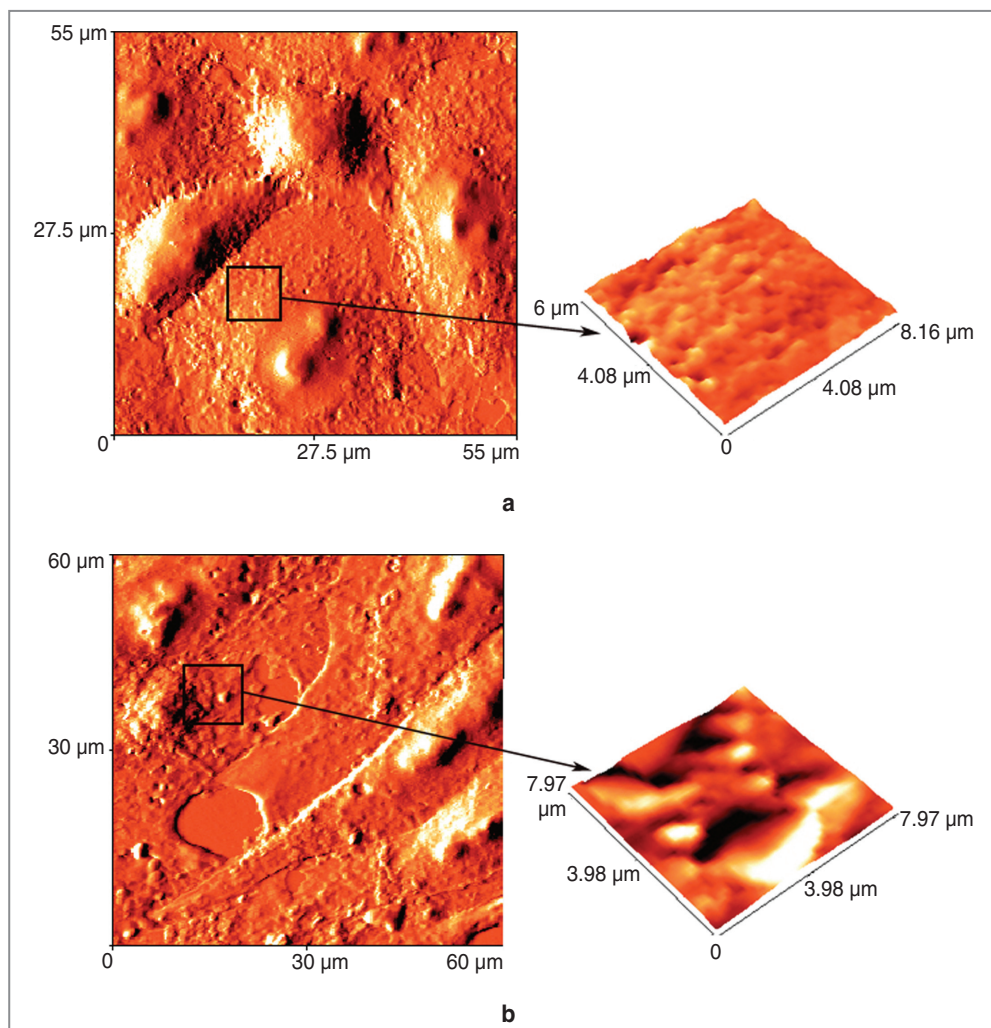


Fig. 4. Atomic-force microscopy of SKOV-3 cells: *a* — control cells; *b* — cells after 6 h of incubation with nanorods, stabilized by Pluronic F127. For the fine details shading at image construction the side illumination was used

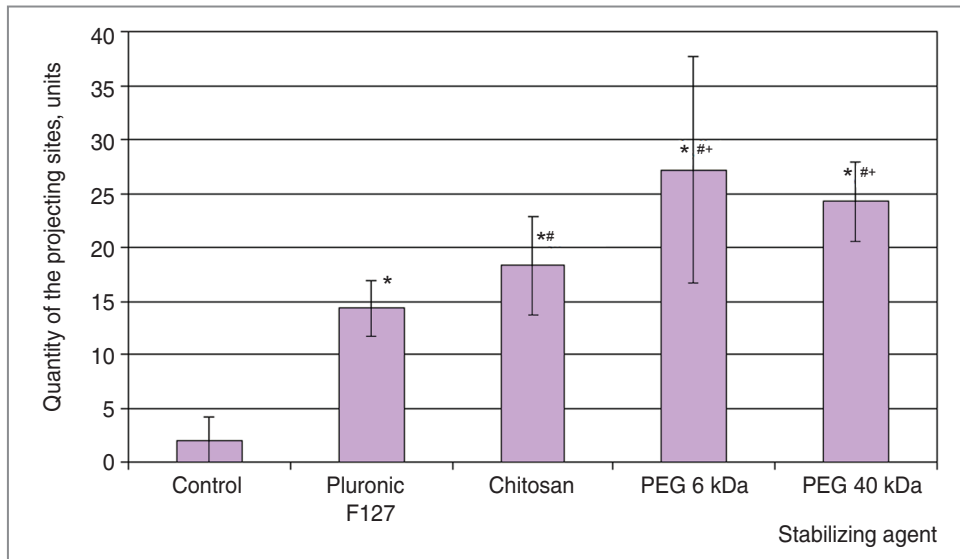


Fig. 5. The quantity of sites projecting over membrane surface. The data significantly differ from the control (*), Pluronic F127 (#) and chitosan (*) at $p < 0.05$

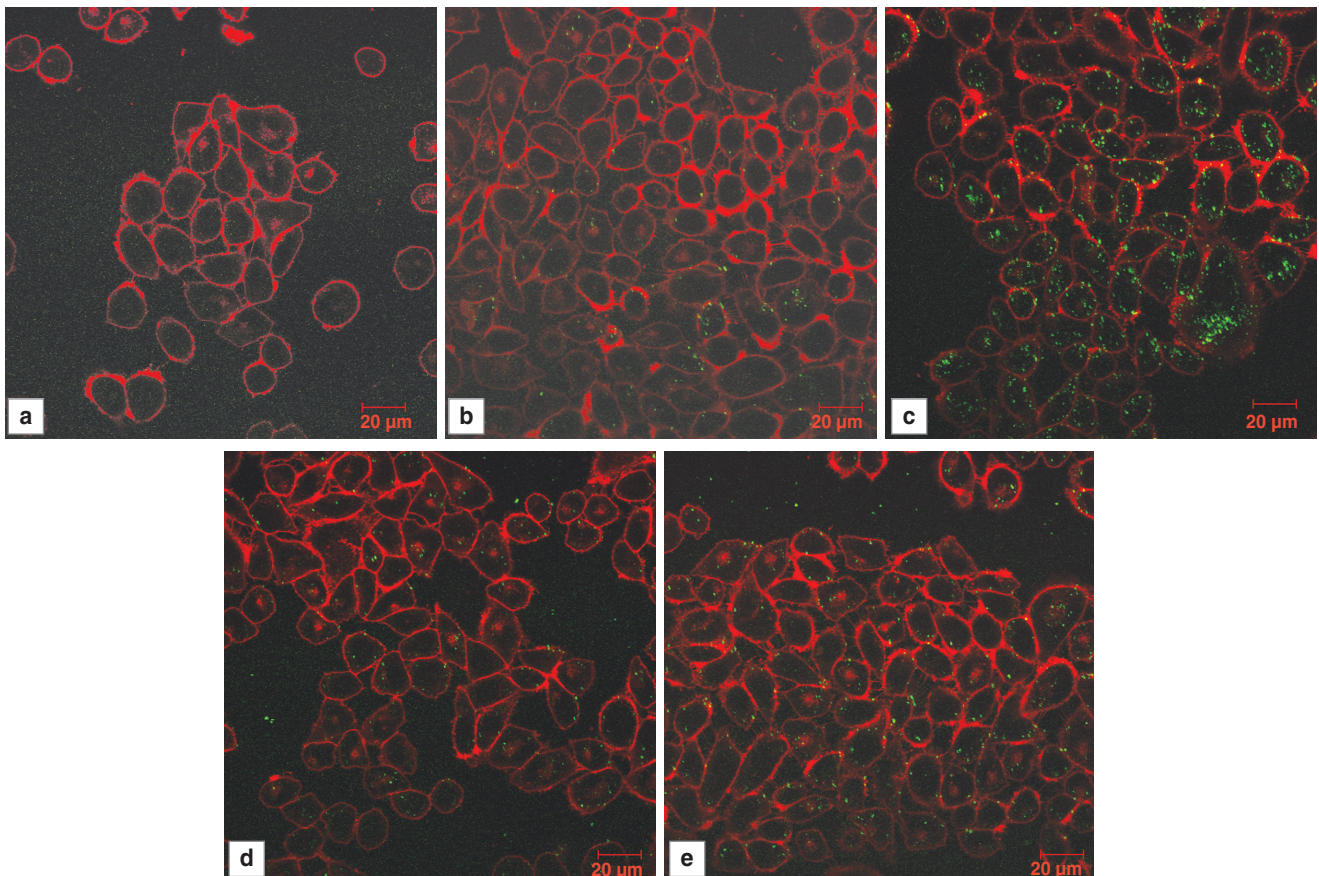


Fig. 6. Two-photon luminescent microscopy of the control cells (a) and cells incubated with the nanoparticles, stabilized by Pluronic F127 (b), chitosan (c), PEG 6 kDa (d), PEG 40 kDa (e). Here and below: the TPLM image is presented as an overlay of the TPLM signal from the nanoparticles (green color) and the signal from the cell membranes (red color)

revealed. The least quantity (14 sites) was observed in the nanoparticles stabilized by Pluronic F127.

Two-photon luminescent microscopy. TPLM showed that the nanoparticles stabilized by chitosan

penetrated into cells most efficiently (Fig. 6). There were more luminescent objects in cells compared to the nanoparticles stabilized by other agents. The nanoparticles stabilized by PEG 40 kDa penetrated into

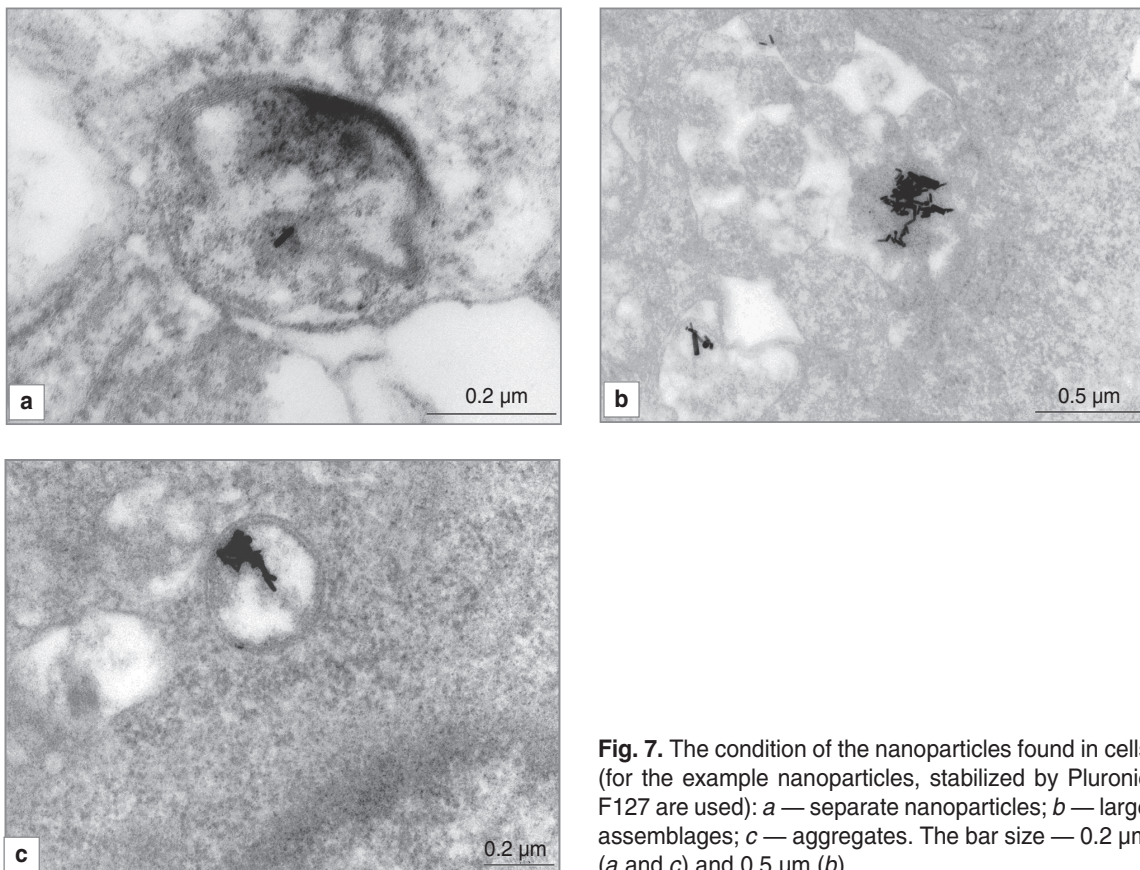


Fig. 7. The condition of the nanoparticles found in cells (for the example nanoparticles, stabilized by Pluronic F127 are used): *a* — separate nanoparticles; *b* — large assemblages; *c* — aggregates. The bar size — 0.2 μm (*a* and *c*) and 0.5 μm (*b*)

cells less efficiently than chitosan stabilized particles. The nanoparticles stabilized by PEG 6 kDa and Pluronic F127 penetrated worse than those stabilized by other agents. The least amount of luminescent objects in cells was recorded in these nanoparticles. All nanorod solutions under study appear to have some common features. The amount of luminescent objects in cells grew with the increase of the incubation time. The majority of the nanoparticles penetrated into cells settled down in the part of a culture plate, which was closer to the bottom.

Transmission electron microscopy. Based on the microphotographs obtained by TEM, the nanoparticles

found in cells were divided into three types: single nanoparticles, large assemblages and aggregates (Fig. 7). Large assemblages of nanoparticles represent groups of a large number of single nanorods located closely to each other. Aggregates are groups of closely packed nanoparticles, inside which single nanoparticles are impossible to separate. It is significant that single nanoparticles were found in cells less frequently than large assemblages of nanoparticles or aggregates. Nanoparticles in cells were registered either free, or surrounded by membrane structures. The presence of a membrane was typical for aggregates and large assemblages of nanoparticles.

After one-hour incubation the amount of the nanoparticles stabilized by PEG 6 kDa and 40 kDa, in cells was higher compared to those stabilized by other agents (See the Table). For example, we revealed 10 large assemblages of nanoparticles for PEG 6 kDa and 28 — for PEG 40 kDa. The number of single nanorods and aggregates was also larger in comparison with chitosan-stabilized and Pluronic-stabilized nanoparticles. The increase of the incubation time was accompanied with the growing number of single nanorods to 14 for PEG 6 kDa and to 12 — for PEG 40 kDa. The

Occurrence of the nanoparticles in cells (data are presented for 20 fields of view)

Type of the nanoparticles	Incubation time, h	Stabilizing agent			
		Pluronic F127	Chitosan	PEG 6 kDa	PEG 40 kDa
Separate nanoparticles	1	2	1	7	6
	3	1	0	5	0
	6	8	6	14	12
Large assemblages	1	5	1	10	28
	3	3	2	6	2
	6	2	5	5	9
Aggregates	1	5	11	12	11
	3	3	21	14	11
	6	18	93	31	44

number of aggregates in cells also increased.

The nanoparticles stabilized by chitosan after one-hour incubation are presented in cells generally as aggregates. After 3 h the quantity of single nanoparticles and large assemblages did not change, and the number of aggregates doubled. The time increase up to 6 h was still associated with growth of a number of aggregates.

The nanoparticles stabilized by Pluronic F127 penetrated into cells in the less amounts. Single nanorods and large assemblages of nanoparticles were found even after 6 h incubation. The number of aggregates in cells grew from 5 to 18 with the increase of the time of interaction from 1 to 6 h.

Endocytosis research. To confirm endocytosis promotes the penetration of nanoparticles into cells, the cells with nanoparticles were incubated for 3 h at low temperature (+4°C). The TPLM-analysis revealed no luminescent objects in cells (Fig. 8). This regularity was exhibited by the nanoparticles stabilized by all studied agents. However, the TEM found single aggregates and large assemblages of the nanoparticles stabilized by Pluronic F127 and chitosan (Fig. 9). PEG-stabilized nanoparticles showed the greatest effectiveness of penetration into cells at low temperature. It is significant that all aggregates and large assemblages of nanoparticles found in cells had no surrounding membrane structures.

Discussion. The nanoparticles used in biomedical researches are coated or stabilized by various agents. On the one hand, a stabilizing agent has to prevent nanoparticles aggregation, on the other hand, it has to minimize the toxicity of nanoparticles. The agents exhibiting specific binding with particular cells or facilitating penetration of nanoparticles into cells are frequently used. However, nanoparticles may change optical properties after stabilization. According to A. Albanese and W.C. Chan [32] there is the shift of the extinction peak of nanoparticles to the long-wave region and its broadening in the process of aggregates formation. This research also demonstrated the broadening of the extinction peak and its shift by

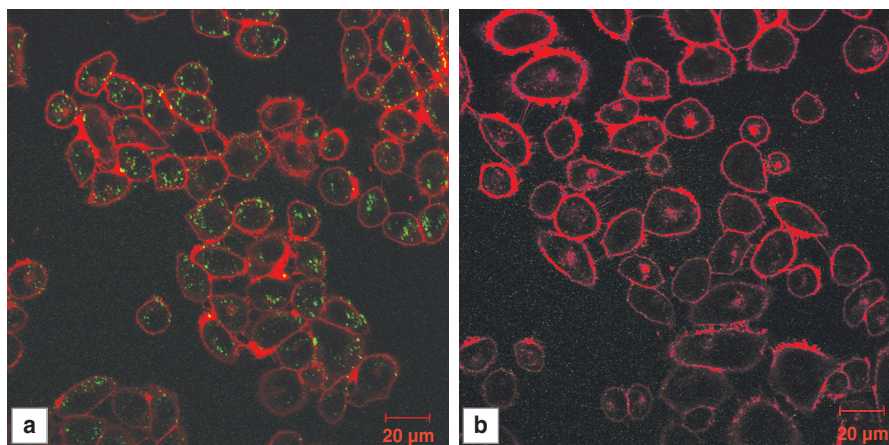


Fig. 8. Two-photon luminescent microscopy of the cells, incubated with nanoparticles, stabilized by chitosan, for 3 h under standard conditions (a) and for 3 h under low temperature — +4°C (b)

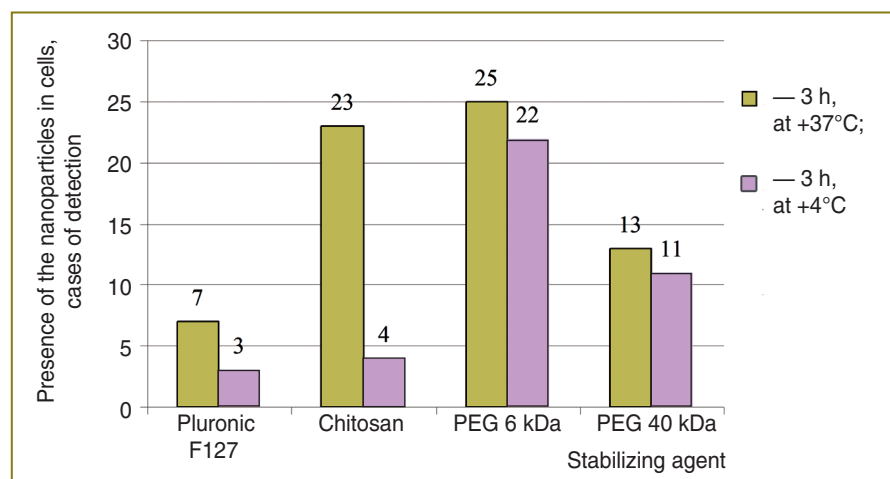


Fig. 9. Occurrence of the nanoparticles in cells after 3 h of the incubation at +4°C and +37°C. The data are presented by summarized quantity of the cases of the separate nanoparticles, large assemblages and aggregates detection in 20 fields of view

30 nm to red spectral range proving the aggregation of nanoparticles in solution. Moreover, we observed the decrease in the peak intensity that could be associated with decreased concentration of nanoparticles in solution (the losses resulted from washing free from CTAB), and with formation of aggregates [33]. Formation of aggregates, on the one hand, is negative because the size of nanoparticles increases resulting in the reduction of their ability to penetrate into cells [13]. On the other hand, nanoparticles as a part of aggregate have higher luminescence intensity due to strengthening [27]. This effect can be used to develop contrasting agents based on plasmon resonance nanoparticles for optical imaging techniques.

According to A.M. Alkilany et al. [34], free CTAB molecules are more toxic for cells than the molecules adsorbed on nanoparticles surface. Authors found out that LD₅₀ for cells treated by free CTAB molecules for 4 days was 200 nmol [34]. In the present research

$5 \cdot 10^{10}$ and $5 \cdot 10^9$ nanoparticles stabilized by CTAB were added to cells that equaled to 270 and 27 nmol of CTAB, respectively, in addition, the cytotoxicity was assessed after 24 h. Probably, for these reasons the decrease in viability appeared to be 30 and 10%, respectively. Analysis of cytotoxicity of the nanoparticles stabilized by other agents revealed no statistically significant differences from the stock solution. However, in the case of PEG-stabilized nanoparticles cells viability was slightly lower that might be due to worse shielding of CTAB molecules remained on nanoparticles surface.

Pluronic was found to facilitate the penetration of comparatively large molecules and large hydrophobic anions through a lipid bilayer [35]. Pluronic is supposed to accelerate the process of solute diffusion within lipid bilayers rather than influencing the rate of solute adsorption/desorption on the membrane surface [14]. However, in the present study, nanoparticles stabilized by Pluronic F127 penetrated into cells worse than the others. It could be due to the fact that removing CTAB from the nanoparticles surface induces the formation of nanoparticle aggregates exceeding the size of Pluronic micelles (30–50 nm).

The nanoparticles stabilized by chitosan penetrated into cells more efficiently after a long period of incubation in comparison with the nanoparticles stabilized by other agents. This result is consistent with other works showing that chitosan may increase cellular transport [17]. Moreover, using of chitosan for nanoparticle stabilization is perspective because chitosan molecules may open the dense contacts and increase the interstitial transport [18]. C. Manaspon et al. [15] noticed that cellular uptake of chitosan-stabilized nanoparticles without surface targets is certain to be mediated by nonspecific adsorption endocytosis. Positively charged nanoparticles stabilized by chitosan can be easily attracted to negatively charged cell membranes and penetrate into cells.

We found the nanoparticles stabilized by PEG 6 and 40 kDa to penetrate well for the first hour, however, with the increase of the incubation period up to 6 h their number inside the cells grew insignificantly. A high accumulation level of nanoparticles during the first hour can be due to the fact that the nanoparticles, which penetrate into cells have on their surfaces PEG molecules, which shield CTAB molecules badly. CTAB is a cationic detergent that increases permeability of membranes [35]. The higher level of cell death after incubation with these nanoparticles could also confirm that fact. Less intensive penetration of nanoparticles into cells after a long-term period may be due to the presence of only well PEG-stabilized nanoparticles in the solution. Such behavior of the nanoparticles may be caused by neutral charge of PEG, and, therefore, nanoparticles interact with cell membrane inactively. The study of C. Freese et al. [25] with primary human dermal microvascular endothelial cells showed that less than 2.5% of initial concentration of the PEGylated gold

nanoparticles penetrated into cells. A similar penetration type was observed for HeLa and PC-3 cells [36].

The significant decrease of the number of the nanoparticles stabilized by Pluronic F127 and chitosan in cells after incubation at low proves the participation of endocytosis in the penetration process. Accumulation of PEG-stabilized nanoparticles in cells did not depend on the temperature and thereby was not associated with endocytosis. These nanoparticles penetrate into cells probably due to unshielded CTAB molecules that increase membrane permeability [35].

Regardless of a stabilizing agent and the time of interaction, the most of the nanoparticles found in cells were large assemblages or aggregates. Most probably, aggregation occurred in the cultural medium due to the interaction of nanoparticles with its components. A.M. Alkilyan and C.J. Murphy [37] showed that proteins from the medium are adsorbed on surface of nanoparticles within 5 min resulting in the change of a charge of nanoparticles and their subsequent aggregation. The presence of proteins on the surface of nanoparticles may also enhance the penetrations of nanoparticles into cells due to receptor-mediated endocytosis [38]. However, culture medium containing different components will differently affect aggregation of nanoparticles and their accumulation in cells [37]. So, C. Fang et al. [39] observed no change of size of iron oxide nanoparticles when added to the phosphate buffered saline, DMEM or fetal bovine serum. Physical and chemical features of a stabilizing agent are likely to be of great importance.

AFM revealed the sites projecting over the membrane surface after 6 h of interaction with nanoparticles. The quantity of such sites was less in Pluronic- and chitosan-stabilized nanoparticles in comparison with PEG-stabilized ones. This may be associated with an interaction of the nanoparticles stabilized by chitosan and Pluronic with membrane and their penetration into cells. The work of R. Guduru [40] has shown that after 3 h of the interaction there are more nanoparticles on the surface of cells than after 6 h. Decrease of quantity of nanoparticles is explained by the author by their penetration into cells. Large number of PEG-stabilized nanoparticles on cell surface could be caused by neutral charge of PEG molecules and their inactive penetration into cells. The same result was shown by TPLM and TEM.

Conclusion. An optimal stabilizing agent for nanoparticles in relation to optical properties preservation is Pluronic. This agent slightly changes extinction spectrum of the gold nanorods solution. Pluronic-stabilized nanoparticles also had the least cytotoxicity. All other studied solutions of nanoparticles including CTAB-stabilized ones show similar cytotoxicity, which is enhanced with the increase of nanoparticles concentration. Two stabilizing agents promoting nanoparticle penetration into cells can be distinguished:

chitosan and PEG. Chitosan-stabilized nanoparticles penetrated well at a long-term period of incubation. Penetration of these nanoparticles is associated with endocytosis. PEG-stabilized nanoparticles penetrated well at early periods of incubation (up to 3 h) including low-temperature conditions.

Study Funding. The work was supported by Ministry of Education and Science, contracts No.14.B25.31.0015 and No.11.G34.31.0017 and by Russian Foundation for Basic Research, contracts No.12-02-31514 and No.12-02-00914.

Conflict of Interests. The authors have no conflict of interests to disclose.

References

1. Astruc D. Transition-metal nanoparticles in catalysis: from historical background to the state-of-the art. In: *Nanoparticles and catalysis*. Edited by Astruc D. Weinheim, Germany: Wiley-VCH Verlag GmbH & Co. KGaA; 2008, <http://dx.doi.org/10.1002/9783527621323.ch1>.
2. Saha K., Agasti S.S., Kim C., Li X.N., Rotello V.M. Gold nanoparticles in chemical and biological sensing. *Chem Rev* 2012; 112(5): 2739–2779, <http://dx.doi.org/10.1021/cr2001178>.
3. Khlebtsov N.G. Optics and biophotonics of nanoparticles with a plasmon resonance. *Quantum Electronics* 2008, 38(6): 504–529, <http://dx.doi.org/10.1070/QE2008v038n06ABEH013829>.
4. Khlebtsov N.G., Dykman L.A. Optical properties and biomedical applications of plasmonic nanoparticles. *J Quant Spectrosc Radiat Transfer* 2010; 111(1): 1–35, <http://dx.doi.org/10.1016/j.jqsrt.2009.07.012>.
5. Stark W.J. Nanoparticles in biological systems. *Angew Chem Int Ed Engl* 2011; 50(6): 1242–1258, <http://dx.doi.org/10.1002/anie.200906684>.
6. Ali Z., Abbasi A.Z., Zhang F., Arosio P., Lascialfari A., Casula M.F., Wenk A., Kreyling W., Plapper R., Seidel M., Niessner R., Knöll J., Seubert A., Parak W.J. Multifunctional nanoparticles for dual imaging. *Anal Chem* 2011; 83(8): 2877–2882, <http://dx.doi.org/10.1021/ac103261y>.
7. Krpetić Z., Nativo P., Sée V., Prior I.A., Brust M., Volk M. Inflicting controlled nonthermal damage to subcellular structures by laser-activated gold nanoparticles. *Nano Lett* 2010; 10(11): 4549–4554, <http://dx.doi.org/10.1021/nl103142t>.
8. Chen J., Glaus C., Laforest R., Zhang Q., Yang M., Gidding M., Welch M.J., Xia Y. Gold nanocages as photothermal transducers for cancer treatment. *Small* 2010; 6(7): 811–817, <http://dx.doi.org/10.1002/smll.200902216>.
9. Phillips M.A., Gran M.L., Peppas N.A. Targeted nanodelivery of drugs and diagnostics. *Nano Today* 2010; 5(2): 143–159, <http://dx.doi.org/10.1016/j.nantod.2010.03.003>.
10. Kang B., Mackey M.A., El-Sayed M.A. Nuclear targeting of gold nanoparticles in cancer cells induces DNA damage, causing cytokinesis arrest and apoptosis. *J Am Chem Soc* 2010; 132(5): 1517–1519, <http://dx.doi.org/10.1021/ja9102698>.
11. von Maltzahn G., Park J.H., Agrawal A., Bandaru N.K., Das S.K., Sailor M.J., Bhatia S.N. Computationally guided photothermal tumor therapy using long-circulating gold nanorod antennas. *Cancer Res* 2009; 69(9): 3892–3900, <http://dx.doi.org/10.1158/0008-5472.CAN-08-4242>.
12. Rozanova N., Zhang J. Photothermal ablation therapy for cancer based on metal nanostructures. *Sci China Ser B: Chem* 2009, 52(10): 1559–1575, <http://dx.doi.org/10.1007/s11426-009-0247-0>.
13. Chithrani B.D., Ghazani A.A., Chan W.C. Determining the size and shape dependence of gold nanoparticle uptake into mammalian cells. *Nano Lett* 2006; 6(4): 662–668, <http://dx.doi.org/10.1021/nl052396o>.
14. Escobar-Chavez J.J., Lopez-Cervantes M., Naik A., Kalia Y.N., Quintanar-Guerrero D., Ganem-Quintanar A. Applications of thermo-reversible Pluronic F127 gels in pharmaceutical formulations. *J Pharm Pharm Sci* 2006; 9(3): 339–358.
15. Manaspon C., Viravaidya-Pasuwat K., Pimpha N. Preparation of folate-conjugated pluronic F127/chitosan core-shell nanoparticles encapsulating doxorubicin for breast cancer treatment. *Journal of Nanomaterials* 2012; Article ID 593878, <http://dx.doi.org/10.1155/2012/593878>.
16. Dumortier G., Grossiord J.L., Agnely F., Chaumeil J.C. A review of poloxamer 407 pharmaceutical and pharmacological characteristics. *Pharm Res* 2006; 23(12): 2709–2728, <http://dx.doi.org/10.1007/s11095-006-9104-4>.
17. Artursson P., Lindmark T., Davis S.S., Illum L. Effect of chitosan on the permeability of monolayers of intestinal epithelial cells (Caco-2). *Pharm Res* 1994; 11(9): 1358–1361.
18. *Chitosan-based systems for biopharmaceuticals: delivery, targeting and polymer therapeutics*. Edited by Sarmiento B., das Neves J. Wiley 2012; 583 p., <http://dx.doi.org/10.1002/9781119962977>.
19. Ahmad M.B., Tay M.Y., Shameli K., Hussein M.Z., Lim J.J. Green synthesis and characterization of silver/chitosan/polyethylene glycol nanocomposites without any reducing agent. *Int J Mol Sci* 2011; 12: 4872–4884, <http://dx.doi.org/10.3390/ijms12084872>.
20. Vasir J.K., Labhasetwar V. Quantification of the force of nanoparticle-cell membrane interactions and its influence on intracellular trafficking of nanoparticles. *Biomaterials* 2008; 29(31): 4244–4252, <http://dx.doi.org/10.1016/j.biomaterials.2008.07.020>.
21. Tapia-Tapia M., Batina N. Nanoscopic characterization of the membrane surface of the HeLa cancer cells in the presence of the gold nanoparticles: an AFM study. *Revista Mexicana de Física S* 2009; 55(1): 64–67.
22. He R.-Y., Su Y.-D., Cho K.-C., Lin C.-Y., Chang N.-S., Chang C.-H., Chen S.-J. Surface plasmon-enhanced two-photon fluorescence microscopy for live cell membrane imaging. *Optics Express* 2009; 17(8): 5987–5997, <http://dx.doi.org/10.1364/OE.17.005987>.
23. Durr N.J., Larson T., Smith D.K., Korgel B.A., Sokolov K., Ben-Yakar A. Two-photon luminescence imaging of cancer cells using molecularly targeted gold nanorods. *Nano Lett* 2007; 7(4): 941–945, <http://dx.doi.org/10.1021/nl062962v>.
24. Peckys D.B., de Jonge N. Visualizing gold nanoparticle uptake in live cells with liquid scanning transmission electron microscopy. *Nano Lett* 2011; 11: 1733–1738.
25. Freese C., Gibson M.I., Klok H.-A., Unger R.E., Kirkpatrick C.J. Size- and coating-dependent uptake of polymer-coated gold nanoparticles in primary human dermal microvascular endothelial cells. *Biomacromolecules* 2012; 13: 1533–1543, <http://dx.doi.org/10.1021/bm300248u>.
26. Coulter J.A., Jain S., Butterworth K.T., Taggart L.E., Dickson G.R., McMahon S.J., Hyland W.B., Muir M.F., Trainor C.,

- Hounsell A.R., O'Sullivan J.M., Schettino G., Currell F.J., Hirst D.G., Prise K.M. Cell type-dependent uptake, localization, and cytotoxicity of 1.9 nm gold nanoparticles. *Int J Nanomedicine* 2012; 7: 2673–2685, <http://dx.doi.org/10.2147/IJN.S31751>.
27. Guan Z., Polavarapu L., Xu Q.H. Enhanced two-photon emission in coupled metal nanoparticles induced by conjugated polymers. *Langmuir* 2010; 26(23): 18020–18023, <http://dx.doi.org/10.1021/la103668k>.
28. Popov V.I., Davies H.A., Rogachevsky V.V., Patrushev I.V., Errington M.L., Gabbott P.L., Bliss T.V., Stewart M.G. Remodelling of synaptic morphology but unchanged synaptic density during late phase long-term potentiation (LTP): a serial section electron micrograph study in the dentate gyrus in the anaesthetized rat. *Neuroscience* 2004; 128(2): 251–262, <http://dx.doi.org/10.1016/j.neurosci.2004.06.029>.
29. Verma A., Stellacci F. Effect of surface properties on nanoparticle–cell interactions. *Small* 2010; 6(1): 12–21, <http://dx.doi.org/10.1002/smll.200901158>.
30. Osaki F., Kanamori T., Sando S., Sera T., Aoyama Y. A quantum dot conjugated sugar ball and its cellular uptake. On the size effects of endocytosis in the subviral region. *J Am Chem Soc* 2004; 126(21): 6520–6521, <http://dx.doi.org/10.1021/ja048792a>.
31. Chithrani B.D., Chan W.C. Elucidating the mechanism of cellular uptake and removal of protein-coated gold nanoparticles of different sizes and shapes. *Nano Lett* 2007; 7(6): 1542–1550, <http://dx.doi.org/10.1021/nl070363y>.
32. Albanese A., Chan W.C. Effect of gold nanoparticle aggregation on cell uptake and toxicity. *ACS Nano* 2011; 5(7): 5478–5489, <http://dx.doi.org/10.1021/nn2007496>.
33. Carroll J.B., Frankamp B.L., Srivastava S., Rotello V.M. Electrostatic self-assembly of structured gold nanoparticle/polyhedral oligomeric silsesquioxane (POSS) nanocomposites. *J Mater Chem* 2004; 14: 690–694, <http://dx.doi.org/10.1039/B311423F>.
34. Alkilany A.M., Nagaria P.K., Hexel C.R., Shaw T.J., Murphy C.J., Wyatt M.D. Cellular uptake and cytotoxicity of gold nanorods: molecular origin of cytotoxicity and surface effects. *Small* 2009; 5(6): 701–708, <http://dx.doi.org/10.1002/smll.200801546>.
35. Vaidyanathan S., Orr B.G., Banaszak Holl M.M. Detergent induction of HEK 293A cell membrane permeability measured under quiescent and superfusion conditions using whole cell patch clamp. *J Phys Chem B* 2014; 118(8): 2112–2123, <http://dx.doi.org/10.1021/jp4124315>.
36. Arnida, Malugin A., Ghandehari H. Cellular uptake and toxicity of gold nanoparticles in prostate cancer cells: a comparative study of rods and spheres. *J Appl Toxicol* 2010; 30(2): 212–217, <http://dx.doi.org/10.1002/jat.1486>.
37. Alkilany A.M., Murphy C.J. Toxicity and cellular uptake of gold nanoparticles: what we have learned so far? *J Nanopart Res* 2010; 12: 2313–2333, <http://dx.doi.org/10.1007/s11051-010-9911-8>.
38. Conner S.D., Schmid S.L. Regulated portals of entry into the cell. *Nature* 2003; 422: 37–44, <http://dx.doi.org/10.1038/nature01451>.
39. Fang C., Bhattarai N., Sun C., Zhang M. Functionalized nanoparticles with long-term stability in biological media. *Small* 2009; 5(14): 1637–1641, <http://dx.doi.org/10.1002/smll.200801647>.
40. Guduru R. *In situ AFM imaging of nanoparticle- cellular membrane interaction for a drug delivery study*. Miami-Florida: FIU Electronic Thesis and Dissertations; 2011.